IRIS: A NEW ERA IN DOWNHOLE DATA TREATMENT

Victoria Pons
Baker Hughes a GE Company

INTRODUCTION

When an oil well stops flowing naturally, artificial lifts methods are needed to stimulate the well's production. One of the most widely used method of artificial lift is reciprocating rod lift. In reciprocating rod lift, a downhole pump is connected to the surface driving mechanism with a rod string. The motion of the prime mover is translated into the vertical motion of the rod string, therefore lifting the production fluids to the surface.

At the surface, a dynamometer and position sensor record the position and load data. Unfortunately, similar recording of downhole position and load data is not commonly available since it requires a downhole dynamometer tool to be placed in the bottom of the rod string.

Historically, reciprocating rod lift wells were initially controlled from the data recorded at the surface. Due to the wide variations of the surface dynamometer cards, this can be a very difficult and unreliable way of controlling a reciprocating rod lift system.

In reciprocating rod lift, work done at the surface is not equal to the work done at the pump.

Because of the elasticity, the rod string will compress and extend as the pumping unit goes up and down. Essentially, the tapered rod string stretches and compresses, as the stress waves, created through the dynamics of pumping cycle, go up and down the rod string at the speed of sound.

Downhole data can be calculated from surface data using the 1-dimensional damped wave equation. The wave equation can then be solved for the downhole data using separation of variables and complex theory [6] or finite differences [5, 9].

The 1-D damped wave equation is given by:

$v_S^2 \frac{\partial^2 u}{\partial x^2} - c\frac{\partial u}{\partial t} = \frac{\partial^2 u}{\partial t^2}.$	1

Due to the viscous friction of the wellbore fluids as well as the friction resulting from deviation, additional energy is continuously and irreversibly lost during the pumping cycle. Because of deviation, mechanical friction decreases the energy available at the pump from the contact between the rods and tubing.

The wave equation models the propagation of stress waves up and down the rod string at the speed of sound. Using the 1D damped wave equation as shown in (1) allows for energy to be removed from the system when calculating downhole data from surface data to mimic the energy lost to viscous forces. Friction originating from viscous forces is proportional to the velocity of the rod string and can therefore be accounted for using the wave equation. This, however is not the case for friction of mechanical origins. Mechanical friction is not accounted for by the wave equation.

After the wave equation was validated as a preferred and reliable way of computing downhole data, downhole data processing has proven to be a more accurate, reliable and robust way of optimizing reciprocating rod lift wells.

The analysis of downhole data can be a difficult depending on the downhole conditions present.

In order to optimize production of a rod pumped well, key control parameters must be extracted from downhole data such as pump fillage, pump intake pressure (PIP), inferred production, etc. These quantities enable the user to make control decisions such as slowing down or stopping the pumping unit to detect fluid pound caused by low pump fillage. The efficiency of the overall pumping unit installation can be assessed enabling the user to make control decision (such as for example installing a different pump, decreasing speed…) to improve their reciprocating rod lift installation, see [3, 4, 7, 8].

An important point to note is that field technicians are responsible for more and more wells. All the methods and algorithm proposed in this invention will enable autonomous control parameter calculation without needing a graphical representation of the downhole card or needing human intervention.

IRIS is built uses logic, statistics, and calculus to make intelligent decision for a robust and accurate calculation of key parameters.

KEY CONTROL PARAMETERS CALCULATED FROM DOWNHOLE DATA.

In order to efficiently control a reciprocating rod lift well, some key control parameters must be extracted from the downhole data as discussed in [10].

As mentioned above, surface data can vary tremendously depending on well conditions, production and pumping unit installation specifics. Even among well with similar downhole conditions, surface data can be drastically different.

Downhole data offers a finite amount of discernable downhole conditions, as shown in Figure 6.

During typical pumping operations, fluids from the wellbore are lifted to the surface at the rate of the pumping speed. Ideally, the pumping unit's speed should be matched with the reservoir conditions and fluid level in order to keep the plunger full. Unfortunately, if a well is pumped too fast, the rate at which the production fluids are extracted from the wellbore is greater than the rate of the reservoir supplying the fluids to the wellbore. This is a condition commonly known as fluid pound or "pumped off". Fluid pound is a downhole condition that should be avoided at all costs. Fluid pound can lead to severe equipment damage that can cost operators thousands of dollars in lost production and equipment replacement and repair.

As can be seen in Figure 1, important key control parameters must be extracted from the downhole data. These key control parameters include but are not limited to netstroke, fluid load, standing valve opening and closing, as well as traveling valve opening and closing, pump horsepower, friction assessment, etc.

Netstroke is an important parameter to calculate since it is directly related to pump fillage. Netstroke is an indication of how filled the plunger is. In order to avoid "pump off" or fluid pound conditions as mentioned above, the pumping unit can be slowed down or stopped for a specific time period, labeled idle time. This idle time allows production fluids to repopulate the wellbore and for the fluid level to rise. Pump fillage is calculated using netstroke and the gross stroke using:

$$PF = \frac{S_N}{S_G}$$	2

Fluid load, and related fluid load lines are essential in excess friction detection, and validation of viscous damping forces present in the well. Along with the netstroke, fluid load can be used to calculate inferred production, efficiency, fluid level, etc. For more details, see [1, 7, 11].

Standing valve opening is essential when estimating unanchored tubing and rod stretch as well as identifying conditions such as worn traveling valve or delayed valve opening. During gas interference, for

example, the top left corner of the downhole card will be rounded and the location of the SVO shifted to the right. This shifted distance represents the un-swept plunger distance due to gas expansion.

Standing valve closing, which typically occurs at the top of stroke TOS, can help calculate pump intake pressure (PIP) and helps detect the presence of extra friction as well as downhole condition such as worn traveling valve or a split barrel.

Traveling valve opening can help calculate pump discharge pressure (PDP).

As previously mentioned, during reciprocating rod lift operations, energy is continuously and irreversibly lost due to friction. This friction can be viscous in nature or mechanical. Viscous friction arises from the productions fluids imparting a viscous force on the outer surface area of the rod string impeding its movement. Energy can be removed from the wave equation using the damping term in equation 1 to mimic the effects of the energy lost to viscous friction during the pumping cycle. Failure to properly estimate and compensate for the viscous friction forces will result in inaccurate downhole data.

Mechanical friction issues from the contact between the rods and the tubing, or the presence of paraffin. Mechanical friction is not accounted for when using the wave equation as seen in equation 1. However, the effects of mechanical friction can be approximated and well control can be modified to accommodate the presence of mechanical friction.

As part of the IRIS algorithm, friction in the downhole card is analyzed. IRIS offers the user new suggested damping factors for both the upstroke or the downstroke for the viscous friction as well as detection system for mechanical friction.

Computing the above-mentioned control parameters is essential for optimizing a reciprocating rod lift well.

DOWNHOLE DATA TRANSFORMATION

IRIS is a series of algorithm for data treatment.

IRIS is comprised of a series of algorithms for data analysis and decision making for reciprocating rod lift wells. IRIS will transform downhole or surface position and load data into polar coordinates. This process enables the program to easily compute key control variables as well as identify downhole conditions present during a pumping unit stroke.

IRIS transforms downhole or surface position and load data into polar coordinates centered at $C_{IRIS}(0.5,0.5)$. Polar coordinates contain radius and reference angle from the center.

This transformation to another coordinate system allows for a simpler, more straightforward and robust way of calculating all the important information needed to optimize a rod pumped well.

The first step in this process is to normalize the data. Normalizing is a very common mathematical process which renders the data comparable to other related data. For instance, fluid loads on reciprocating rod lift installation vary with depth, size of pump, pumping speed, viscosity of the production fluids…. The peak polished rod load and minimum polished rod load can also vary greatly between wells. Let $P(x)$ denote downhole position data and $L(x)$ denote the downhole load data.

Normalizing the data enables IRIS to produce comparable data sets for any well regardless of the above-mentioned parameters.

In order to normalize the data, the position and load data are divided by their respective spans. This creates a normalize position and load data sets ranging from [0, 1], as shown in Figure 3.

$$For\ i = 1, \dots, N:$$

$$NP(x) = \frac{P(x)}{R_P}, and\ NL(x) = \frac{L(x)}{R_L}.$$

The polar coordinates center is (0.5,0.5), this involves a change in coordinates. Every point of the normalized data set is shifted to have $C_{IRIS}(0.5,0.5)$ as the center of the new coordinate system.

$$\forall (x, y) \ni x \in P(x)\ \&\ y \in L(x),$$

$$P_{IRIS} = (x - 0.5. y - 0.5).$$

From calculus, polar coordinates describe points in space using a radius and a reference angle to the origin.

The radius data is simply taken to be the distance between the normalized point and the origin, while the reference angle is the angle in radians or degrees between the normalized shifted point and the horizontal line $y = 0.5$ passing through the coordinate system origin $C_{IRIS}(0.5,0.5)$ as seen in Figure 4.

The radius is calculated using the traditional distance formula:

$$R_C = \sqrt{(x - 0.5)^2 + (y - 0.5)^2}.$$

The reference angle is calculated using:

$$\theta_C = \tan^{-1}\frac{y}{x}.$$

APPLICATION OF RADIUS DATA SET.

The radius data set can be analyzed to identify standing valve opening and closing, traveling valve opening and closing, top of stroke and pump fillage.

As can be seen from Figure 7, the local and absolute maximums of the radius data set correspond to the valve openings and closings. From Calculus, the four sides and four corners of the card correspond to the absolute and local minimum and maximum of the radius data set respectively.

By computing the first derivative of the radius data set and finding the critical points, one can calculate the location of the different above-mentioned events.

Additionally, computing the second derivative of the radius data set and finding points of inflection allows for an accurate way of identifying the key events on the downhole card.

Let $R_C(x)$ denote the radius data set.

The first and second derivative can be calculated using traditional methods for discrete data sets.

From Calculus, critical points for the radius data can be calculated by solving $R_C'(x) = 0$. Inflection points can be calculated by solving $R_C''(x) = 0$. For each critical point, if $R_C{}'(x)$ changes from positive to negative, then $R_C(x)$ has a local maximum. If $R_C{}'(x)$ changes from negative to positive, then $R_C(x)$ has a local minimum. If $R_C''(x) > 0$, then the function $R_C(x)$ is concave up. If $R_C''(x) < 0$, then the function $R_C(x)$ is concave down, whereas if changes from positive to negative, then $R_C(x)$ has a local maximum.

Radius data sets can be directly compared and contrasted to ideal radius data set by using techniques such as least squares or statistical deviation, see [2] from the original current card signal, see section VI.

APPLICATION OF REFERENCE ANGLE DATA SET.

As mentioned above the reference angle data is the angle between the normalized shifted point to the origin of the coordinate system $C_{IRIS}(0.5,0.5)$ as seen in Figure 2.

The reference angle data set gives information on the spatial location of the normalized point with respect to the above-mentioned center.

Reference angles belonging to [150°, 200°] corresponds to the rod stretching as it is lifted by the pumping unit on the upstroke. Reference angles belonging to [30°, 150°] corresponds to the part of the upstroke when the plunger moves up. Reference angles belonging to [340°, 30°] corresponds to the rods compressed back to their original state during the downstroke, while reference angles belonging to [210°, 330°] corresponds to the rest of the downstroke as the plunger moves back to its original position as seen in Figure 2.

The reference angle data set also enable data treatment per sector. The card can be analyzed sector by sector with increments as small as 1°.

The reference angle data set allows for the data to be parted by specific events as explained in the last paragraphs, which can greatly simplify and speed up data treatment.

For instance, for a well with more than 50% pump off, this can easily be seen by the absence of data points for reference angles [270°, 360°]. The radius and reference angle data set can therefore help guide the calculation of key parameters, which would be difficult to find mathematically.

Another application of the reference angle data set is the ability to look at the point distribution per angle sector. IRIS polar coordinate points can be sorted by any angle increment (θ_S = 5°, 10°, 15°…) for coarser or finer results.

The sorted points can now create a probability density function, which accentuates the areas of the downhole card having the highest point concentrations, as shown in Figure 5.

When there is an accumulation of points in the downhole data, this indicates that the rod string slowed down at that particular point. This slowing down phenomenon can be attributed to either normal pumping operations, i.e. the pumping unit will slow down at the top of stroke and at the bottom of stroke as well as slightly slow down after the rods are stretched and after they are compressed back into their normal size.

The accumulation of points can also be attribute to a wellbore event such as a moderate to severe dog leg.

Comparing the position of the slowing down relative to rod stretch can pin point exact location of where the rods are “sticking”, meaning that either due to deviation or paraffin or trash, the rod string is slowed down or stopped momentarily. Using that information, the depth of the event can be calculated using the coefficient of rod stretch.

This can be a crucial step in understanding the effects of deviation on the rod string and the different sources of extra friction and their impact on day to day operations.

IDEAL CARDS

Since the validation of wave equation, different conditions can be easily identified from the downhole dynamometer card such as full pump, unanchored tubing, fluid pound, gas interference, tagging, standing valve wear, traveling valve wear, or extra friction present as seen in Figure 6.

In the oil and gas industry, it is common practice to refer to these or similar ideal cards for given downhole conditions. An ideal card typically will display one downhole condition per card or a combined condition

such as fluid pound and traveling valve wear for example. To that effect the concept of pattern matching per sector is an effective tool to diagnose and optimize a downhole well.

Additionally, understanding the downhole conditions present during the pumping cycle of a particular well can give some insight as to better optimize production and also can guide the accurate and reliable calculation of key control parameters.

When processing these ideal cards with IRIS, this gives rise to ideal downhole condition polar coordinate data and computed parameters. This means that each position and load ideal data point is now converted and therefore comparable to IRIS polar coordinates of other cards.

This comparison can take the shape of comparing trends of the radius data set between ideal data and current data. The reference angle data set can also be compared to give some insight on the downhole condition present.

Using the newly created radius, reference angle and corresponding probability density function, current cards can be compared with ideal cards' radius, reference angle and probability density function per sector. Least squares and other mathematical techniques, see [2] can be used to assess the degree of compatibility between the current data and ideal data using:

$$E(x) = \sum \left[R_{C\_current} - R_{C\_ideal}\right]^2.$$

Not only does this method speed up the convergence of the analysis, but it also makes it possible and feasible to test different downhole conditions in the same card.

For example, for any particular sector, the behavior of the current card can be compared using the above data set to an entire library of ideal card capable of returning a percentage of certainty for certain downhole conditions to be present. This enables the diagnosis of multiple downhole conditions in the same card.

FRICTION ASSESSMENT

As mentioned above, during the pumping cycle, energy is continuously and irreversibly lost due to friction.

IRIS evaluates the amount of viscous friction and mechanical friction present for a given stroke for any well. Using the calculated valve opening and closing, the fluid load lines $F0_{DOWN}$ and $F0_{UP}$ can be computed.

The area between the top of downhole card and $F0_{UP}$ as well as the area between the bottom of the card and $F0_{DOWN}$ are computed using Riemann sums. The equation for the upstroke and downstroke areas (UA and DA) is given by:

$$UA = \sum_{n=0}^{k-1} [f(x_n) - F0_{UP}] \cdot \Delta x,$$	3

and

$$DA = \sum_{n=0}^{k-1} [F0_{DOWN} - f(x_n)] \cdot \Delta x.$$	4

Ideally, in the absence of mechanical friction, the pump horsepower should equal the hydraulic horsepower.

When the pump horsepower is greater than the hydraulic horsepower, either there is mechanical friction present in the downhole data and/or the viscous damping term of the wave equation did not remove enough energy to compensate for the viscous forces present in the well.

The hydraulic horsepower can be calculated as described in [1] using:

$$HP_{HYD} = 7.36 \cdot 10^{-6} \cdot q \cdot \gamma_L \cdot FL_W.$$	5

When the pump horsepower is smaller than the hydraulic horsepower, too much energy was removed from the wave equation when calculating downhole data. IRIS provides a suggested upstroke damping factor as well as a downstroke damping factor. These damping factors can be used as part of an iterative process as the iteration on damping proposed by Everitt-Jennings in [5].

IRIS provides a way of evaluating appropriate viscous damping coefficients as well as diagnose the presence of mechanical friction in the downhole data. Being able to recognize the presence of mechanical friction and control the well accordingly essential for our users to minimize failures, downtime and lost production.

In the next section, results are presented.

RESULTS

IRIS was applied to several data sets. Results from a full card example are displayed in Figure 7.

The normalized downhole card is displayed on the top left. The position and load downhole data is normalized and therefore belong to [0, 1]. The normalized non-dimensional position data is displayed on the top right.

The reference angle data set is displayed on the middle right, while the radius data set is displayed on the middle left.

The first and second derivatives of the radius data set are displayed on the bottom left and right graphs respectively.

The radius data set curve is analyzed to find the location of the valve openings and closing through Calculus. The valve closing/opening are characterized by the local and absolute maximums from the radius data. Once IRIS has identified the points whose polar coordinates correspond to the valves opening and closing, using the same index, the non-dimensional coordinates for that same point can be multiplied by the downhole position and load spans respectively to yield the original downhole data point corresponding to the valve opening or closing.

The results from the pattern matching indicate a full pump.

For the full card example, the polar coordinates of the SVO are (0.67, 137°), the non-dimensional coordinates of the SVO are (0.0412, 0.9898). The polar coordinates of the SVC are (0.64, 42°), the non-

dimensional coordinates of the SVC or TOS are (0.9761, 0.9321). The polar coordinates of the TVO are (0.62, 318°), the non-dimensional coordinates of the TVO are (0.9719, 0.0868). The polar coordinates of the TVC are (0.66, 222°), the non-dimensional coordinates of the TVC are (0.0164, 0.0505).

The location of the openings and closing is then be verified using the reference angle and probability density function of the point distribution per sector. The sector increment can be increased or decreased for finer analysis.

Several methods for the calculation of pump fillage are required to ensure exact calculation of the variable. As mentioned above, due to variety of downhole condition and corresponding downhole card, the use of one method is unadvisable and inaccurate. IRIS contains four different methods for pump fillage calculation to guarantee correct estimation of the pump fillage.

The linear behavior of the points between the SVC/TOS and TVO can be analyzed to calculated pump fillage, using statistics or other methods. In one example, the normalized position values between TOS and TVO can be average to give a pump fillage value of 99.0% as shown by Method 4.

The $F0_{UP}$ line is set at the SVC/TOS at 9321 lbs., while $F0_{DOWN}$ line is set at the TVO at 868 lbs. The calculated fluid load for the full card example is 8453 lbs.

Using Riemann sums or other method, to approximate the amount of extra friction present or to assess the accuracy of the viscous damping, IRIS suggests no change in viscous damping and does not detect the presence of mechanical friction.

In Figure 8, results from an anchored pumped off well are presented. The results from the pattern matching indicate anchored tubing and pumped off condition. The polar coordinates of the SVO are (0.6294, 136°), the non-dimensional coordinates of the SVO are (0.071, 0.975). The polar coordinates of the SVC are (0.6852, 48°), the non-dimensional coordinates of the SVC or TOS are (0.988, 0.981). The polar coordinates of the TVO are (0.5144, 306°), the non-dimensional coordinates of the TVO are (0.803, 0.084). The polar coordinates of the TVC are (0.6532, 226°), the non-dimensional coordinates of the TVC are (0.051, 0.024).

The final pump fillage value computed by IRIS shows 85.34%. The $F0_{UP}$ line is set at the SVC/TOS at 9358 lbs., while $F0_{DOWN}$ line is set at the TVO at 848 lbs. The calculated fluid load for the full card example is 8510 lbs. IRIS suggests an increase in upstroke and downstroke damping factor. This means that not enough energy was removed from the system when solving the wave equation.

In Figure 9, results from a well with mild gas interference are presented. The results from the pattern matching indicate mild gas interference. The polar coordinates of the SVO are (0.632, 136°), the non-dimensional coordinates of the SVO are (0.026, 0.950). The polar coordinates of the SVC are (0.6858, 43°), the non-dimensional coordinates of the SVC or TOS are (0.995, 0.973). The polar coordinates of the TVO are (0.5491, 308°), the non-dimensional coordinates of the TVO are (0.844, 0.072). The polar coordinates of the TVC are (0.6705, 222°), the non-dimensional coordinates of the TVC are (0.00, 0.044).

The final pump fillage value computed by IRIS shows 87%. The $F0_{UP}$ line is set at the SVC/TOS at 9730 lbs., while $F0_{DOWN}$ line is set at the TVO at 720 lbs. The calculated fluid load for the full card example is 9010 lbs. IRIS suggests no change in damping factor as no excess friction is detected.

In Figure 10, results from a well with severe gas interference are presented. The results from the pattern matching indicate severe gas interference. The polar coordinates of the SVO are (0.590, 134°), the non-dimensional coordinates of the SVO are (0.085, 0.91). The polar coordinates of the SVC are (0.6459, 43°), the non-dimensional coordinates of the SVC or TOS are (0.968, 0.945). The polar coordinates of the TVO are (0.465, 253°), the non-dimensional coordinates of the TVO are (0.367, 0.054). The polar coordinates of the TVC are (0.6136, 223°), the non-dimensional coordinates of the TVC are (0.055, 0.077).

The final pump fillage value computed by IRIS shows 36.72%. The $F0_{UP}$ line is set at the SVC/TOS at 8668 lbs., while $F0_{DOWN}$ line is set at the TVO at 540 lbs. The calculated fluid load for the full card example is 8128 lbs. IRIS suggests an increase in upstroke damping factor as excess friction is detected.

In Figure 11, results from a well with fluid acceleration are presented. The results from the pattern matching indicate severe fluid acceleration. The polar coordinates of the SVO are (0.6262, 129°), the non-dimensional coordinates of the SVO are (0.098, 0.980). The polar coordinates of the SVC are (0.4910, 344°), the non-dimensional coordinates of the SVC or TOS are (0.973, 0.371). The polar coordinates of the TVO are (0.66, 318°), the non-dimensional coordinates of the TVO are (0.997, 0.055). The polar coordinates of the TVC are (0.6417, 219°), the non-dimensional coordinates of the TVC are (0.006, 0.089).

The final pump fillage value computed by IRIS shows 100%. The $F0_{UP}$ line is set at the SVC/TOS at 3715 lbs., while $F0_{DOWN}$ line is set at the TVO at 554 lbs. The calculated fluid load for the full card example is 3161 lbs. IRIS suggests no change in damping factor. IRIS suggests decreasing pumping speed.

CONCLUSIONS

IRIS is a comprehensive self-learning algorithm, which offers reliable, robust and accurate calculation of key control parameters necessary for reciprocating rod list optimization.

This innovative method creates three new data sets (radius, reference angle and probability density function) by changing the point of reference from outside the downhole card to inside the card centered at the center of the circumscribed circle of radius $\frac{\sqrt{2}}{2} = 0.707$.

IRIS calculates key control parameters such as pump fillage, fluid load, valve openings and closing as well as provides an assessment of the friction present during the stroke. When users are responsible for thousands of wells, it is important to have autonomous method, which to not require human intervention.

IRIS opens a new era for downhole data analysis through never seen before data sets and techniques.

Glossary of Terms

PIP	Pump Intake Pressure, psi	P_{IRIS}	Point shifted to new center
PDP	Pump Discharge Pressure, psi	θ_C	Reference angle data set, degrees
NP(x)	Normalized positions, nd	R_C	Radius data set, nd
NL(x)	Normalized loads, nd	PF	Pump Fillage, %
P(x)	Position Data, inches	S_N	Net stroke, inches
L(x)	Load Data, lbs	S_G	Gross stroke, inches
R_P	Range of position data , inches	v_S	Velocity of sound, ft/s
R_L	Range of load data, lbs	$\frac{\partial^2 u}{\partial x^2}$	Second derivative of rod displacement over rod length
$\frac{\partial u}{\partial t}$	First derivative of position with respect to time. Rod string element velocity, ft/s	$\frac{\partial^2 u}{\partial t^2}$	Second derivative of position with respect to time. Rod string element acceleration, ft/s^2
c	Damping factor, nd	$R'_C(x)$	First derivative with respect to time of radius data set
$R''_C(x)$	Second derivative with respect to time of the radius data set	E(x)	Error from least square analysis
K_r	Coefficient of rod stretch	A	Area of rod, sq. in.
E	Youngs modulus of elasticity of rod	L	Length of rod, ft
UA	Upstroke Area, in^2	DA	Downstroke Area, in^2
$R_{C-current}$	Radius data set for current card	$R_{C-ideal}$	Radius data set for ideal card
$F0_{down}$	Downstroke fluid load line, lbs	$F0_{up}$	Upstroke Fluid load lines, lbs
$F0$	Fluid load, lbs	Δx	Rod string increment length, inches
HP_{HYD}	Hydraulic horsepower, hp	q	Liquid production rate, STB/day
γ_L	Liquid specific gravity, nd	FL_W	Depth to working fluid level, ft

Bibliography and Prior Art

1. Bommer P., Podio A.L., “The Beam Lift Handbook”, PETEX 2012
2. Burden R. L., Faires J. D., “Numerical Analysis”, 7th edition 2001
3. Ehimeakhe V. M., “Calculation of Downhole Pump Fillage and Control of Pump based on said fillage”, US 20110091332
4. Ehimeakhe V. M., Booth K., “Calculation of Downhole Pump Fillage and Control of Pump based on said fillage”, US 20110091335
5. Everitt T.A., Jennings J.W., “An Improved Finite-Difference Calculation of Downhole Dynamometer Cards for Sucker-Rod Pumps.”, SPE 18189, 1992.
6. Gibbs S.G., “Rod Pumping”, 2012
7. Pons V. M., “Fluid Load Line calculation and concavity test for downhole pump card”, US 9810212
8. Pons V. M., Allison, A. P., Gomes, J. M. “Diagnostics of Downhole Dynamometer Data for Control and Troubleshooting of reciprocating Rod Lift Systems” US20170016313
9. Pons-Ehimeakhe, V. M., “Modified Everitt-Jennings Algorithm with dual iteration on damping factors”, South Western Petroleum Short Course, Lubbock, TX 2012.
10. Rowlan L. O. et. al., “Pump Intake Pressure Determined from Fluid Levels, Dynamometers, and Valve Test Measurements”, Paper 2009-170, Canadian International Petroleum Conference, Alberta, Canada, 16-18 June 2009.
11. Takacs G., “Sucker Rod Pumping Manual”, PennWell 2003

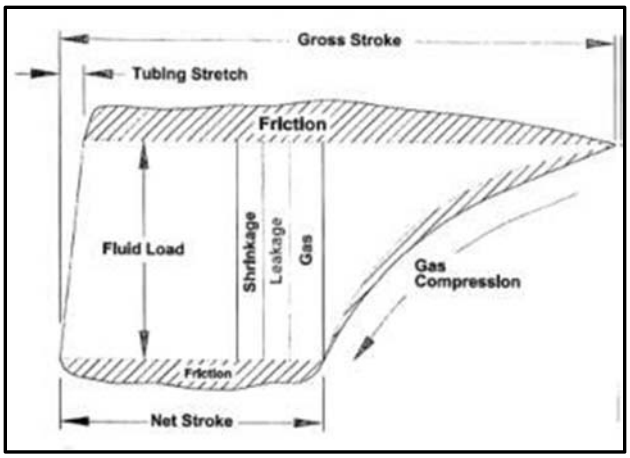

Figure 1: Dynamometer Card Interpretation.

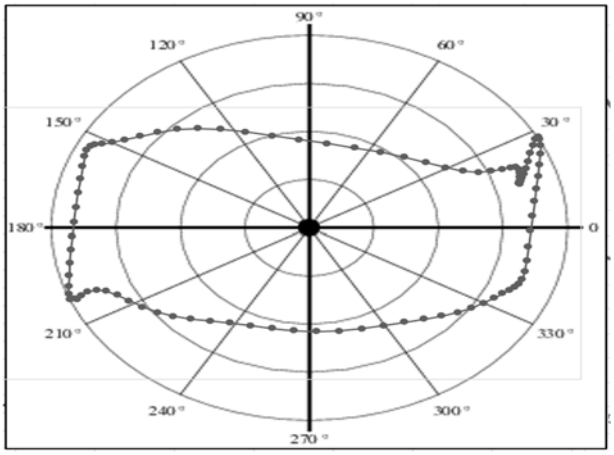

Figure 2: IRIS overview.

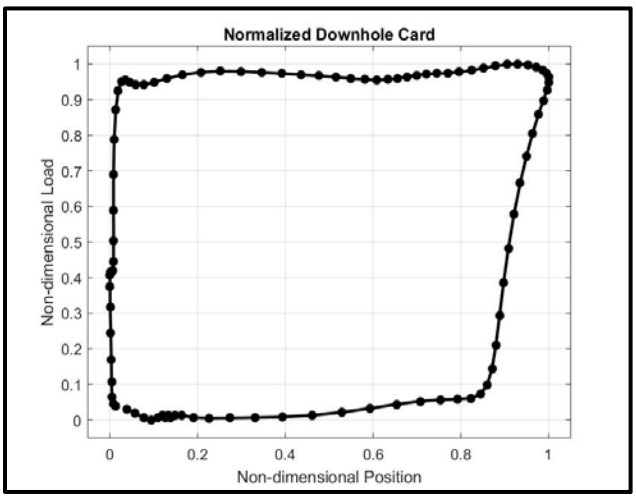

Figure 3: Normalized Downhole Card.

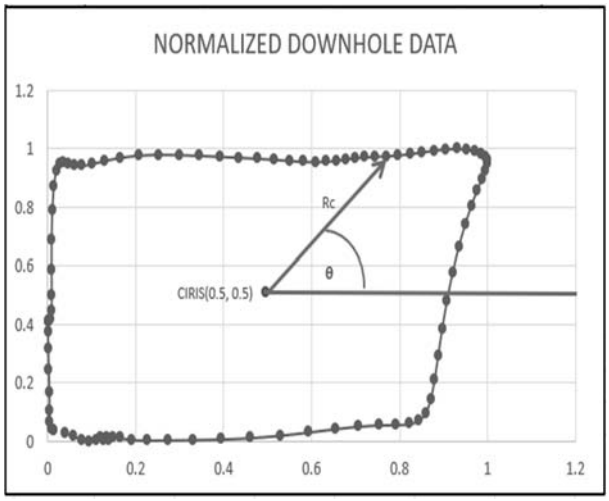

Figure 4: IRIS Polar Coordinate description

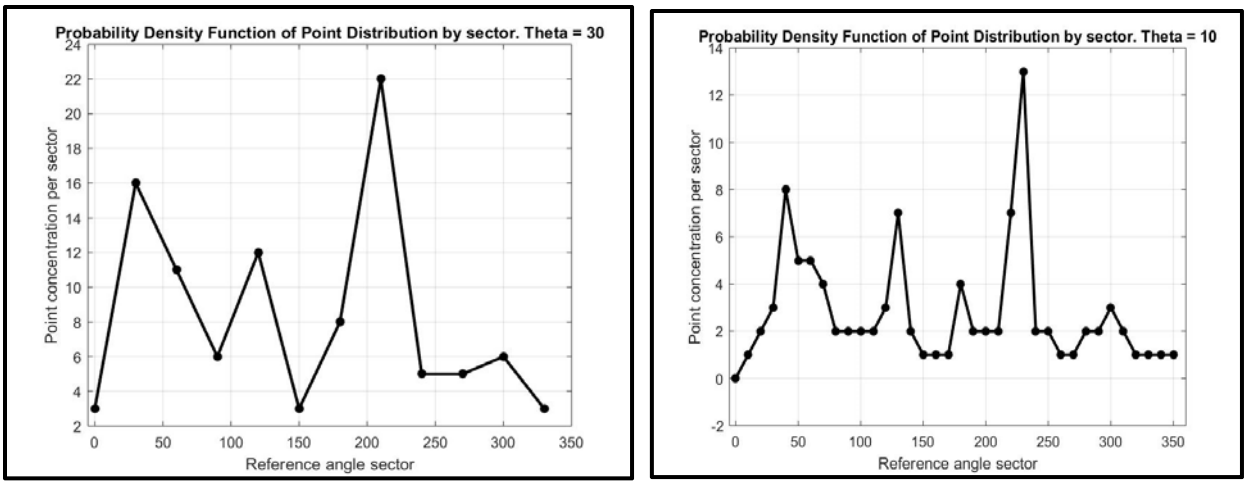

Figure 5: Probability Density Function for Point Distribution with different angle increments: (left) 30° and (right) 10°.

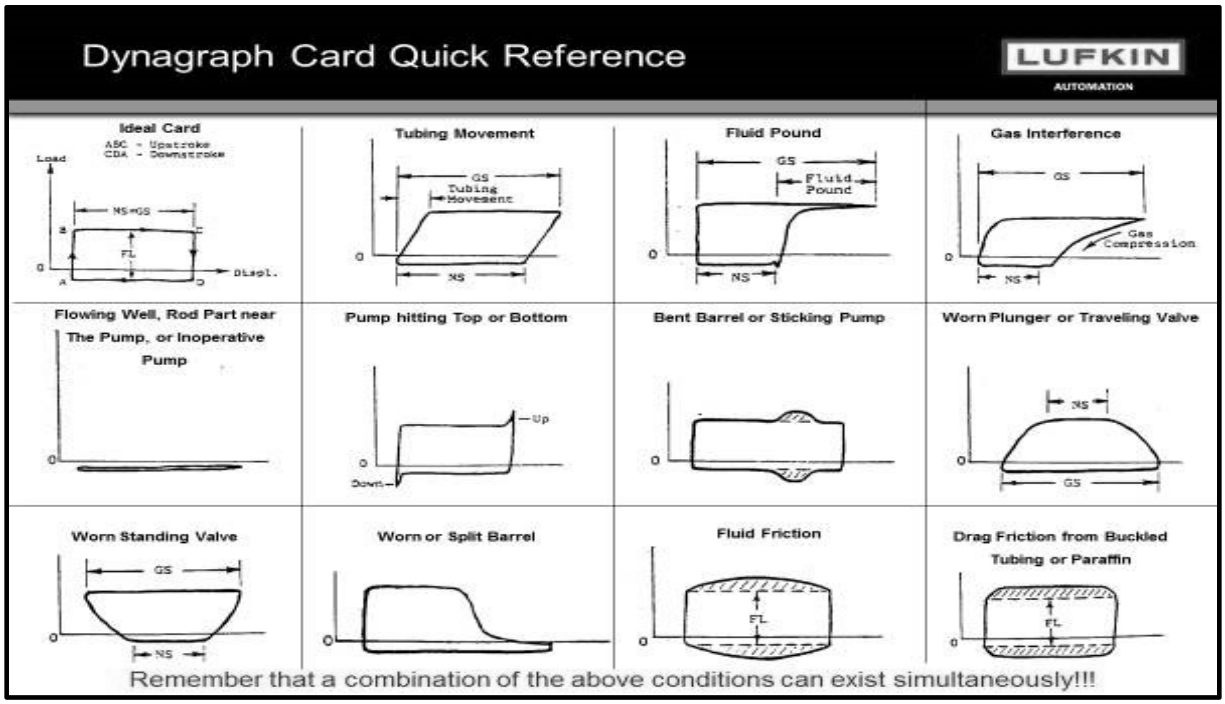

Figure 6: Downhole Dynamometer Card Reference: Ideal Cards.

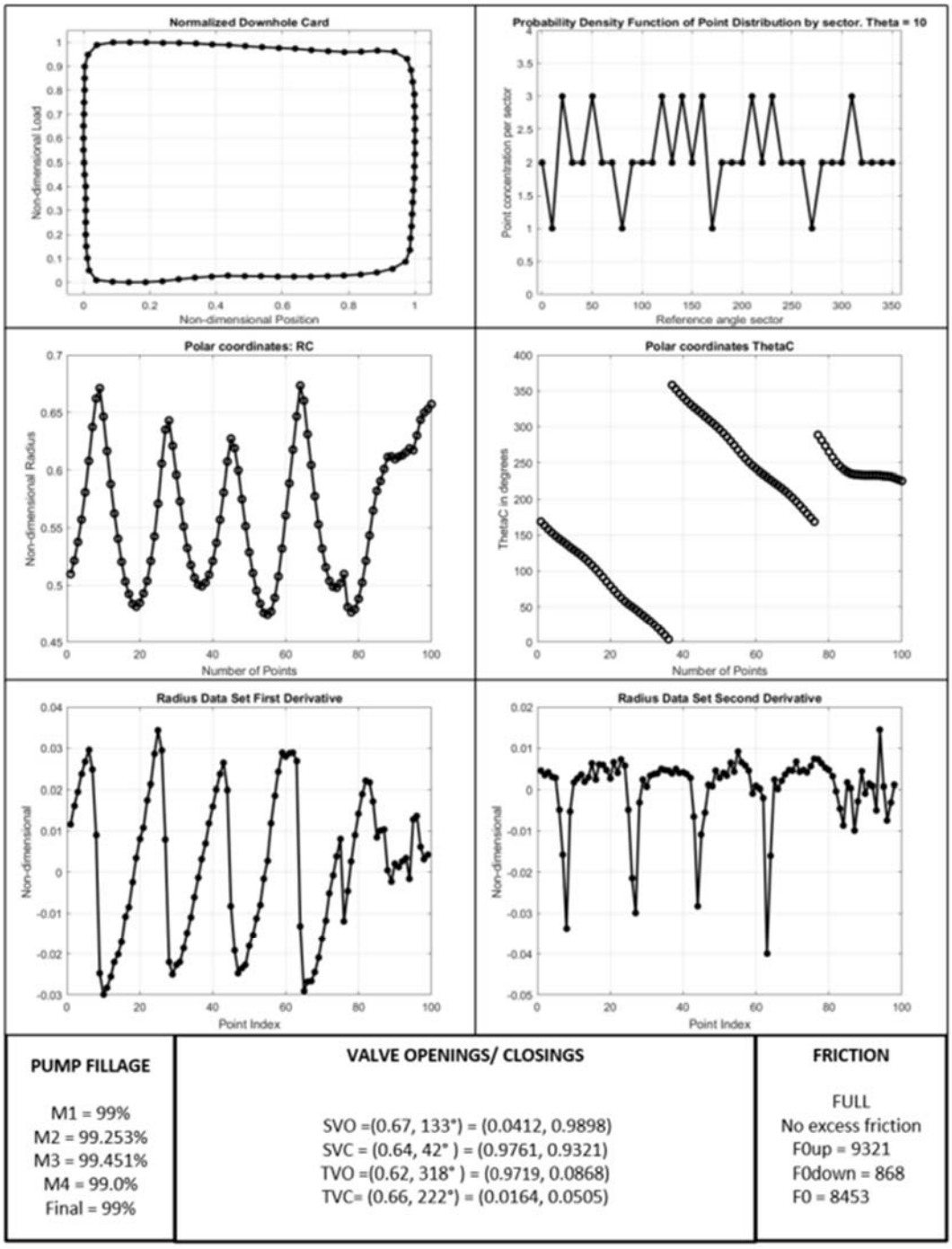

PUMP FILLAGE	VALVE OPENINGS/ CLOSINGS	FRICTION
M1 = 99% M2 = 99.253% M3 = 99.451% M4 = 99.0% Final = 99%	SVO =(0.67, 133°) = (0.0412, 0.9898) SVC = (0.64, 42°) = (0.9761, 0.9321) TVO =(0.62, 318°) = (0.9719, 0.0868) TVC= (0.66, 222°) = (0.0164, 0.0505)	FULL No excess friction F0up = 9321 F0down = 868 F0 = 8453

Figure 7: IRIS Results: Full Card Example 1

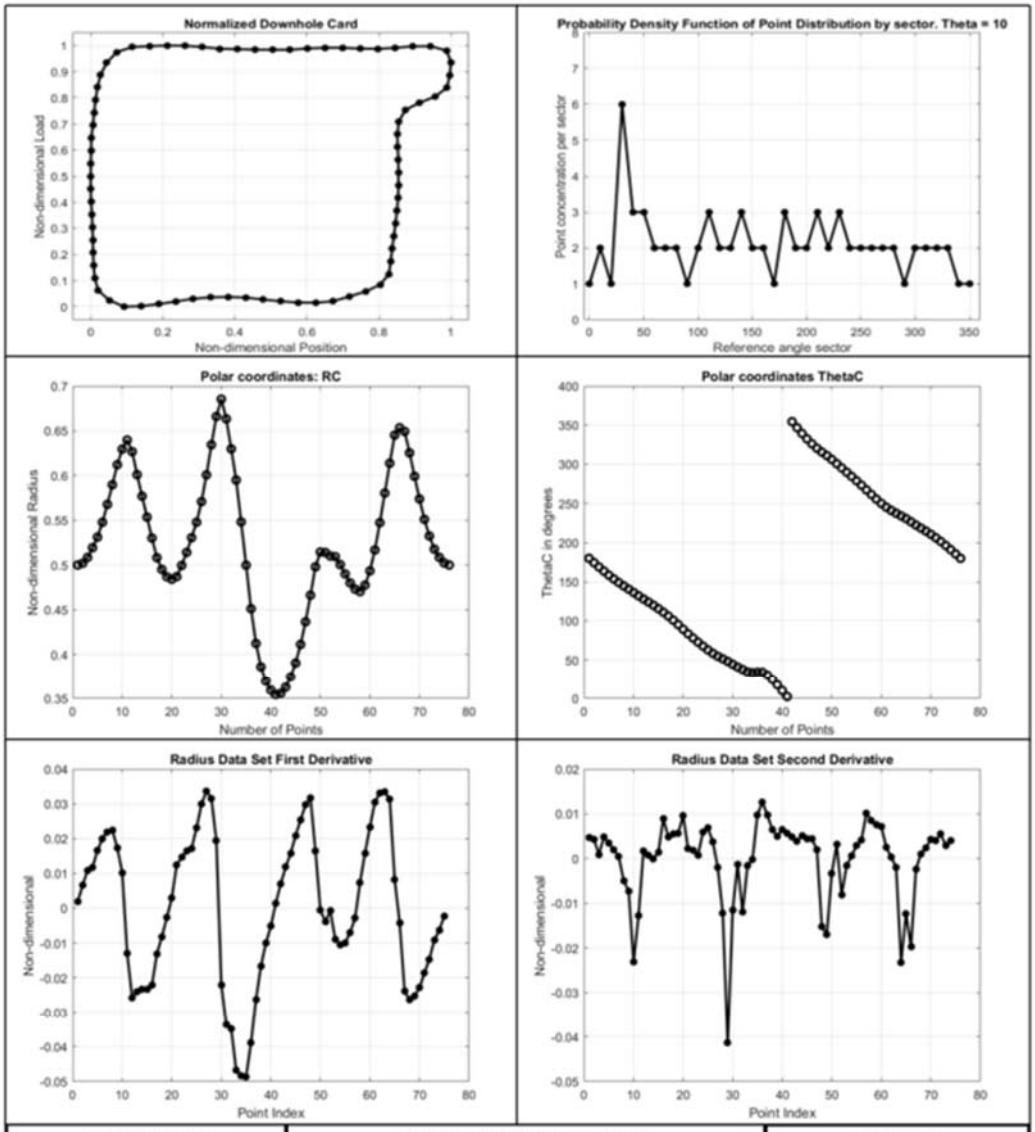

PUMP FILLAGE	VALVE OPENINGS/CLOSINGS	FRICTION
M1 = 85.40	SVO = (0.6294, 136°) = (0.071, 0.975)	APO
M2 = 88.22	SVC = (0.6852, 48°) = (0.988, 0.981)	Increase Viscous Damping
M3 = 85.11	TVO = (0.5144, 306°) = (0.803, 0.084)	F0up = 9358
M4 = 85.51	TVC= (0.6532, 226°) = (0.051, 0.024)	F0down = 848
Final = 85.34		F0 = 8510

Figure 8: IRIS Results: Anchored Pumped Off Example 2

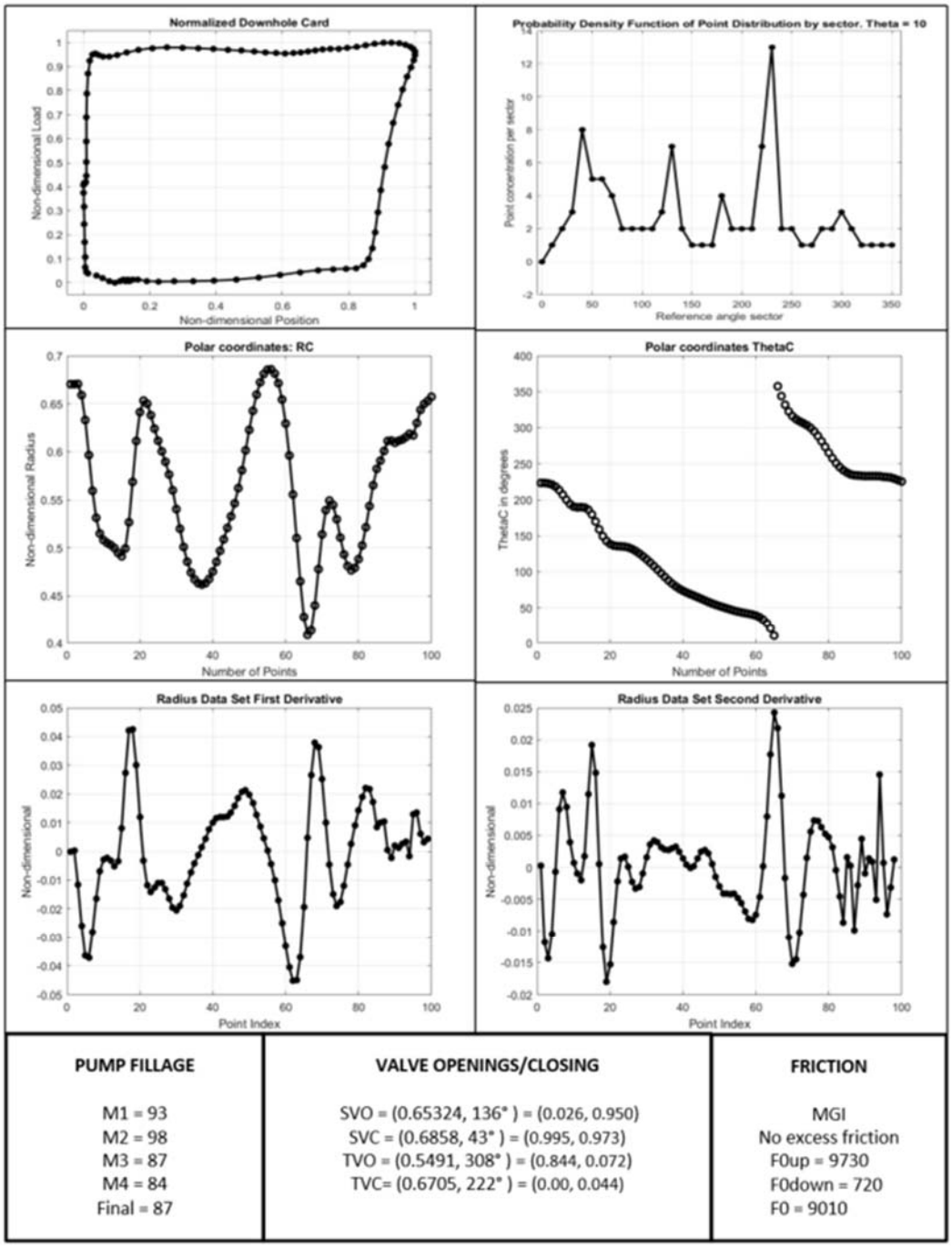

PUMP FILLAGE	VALVE OPENINGS/CLOSING	FRICTION
M1 = 93 M2 = 98 M3 = 87 M4 = 84 Final = 87	SVO = (0.65324, 136°) = (0.026, 0.950) SVC = (0.6858, 43°) = (0.995, 0.973) TVO = (0.5491, 308°) = (0.844, 0.072) TVC= (0.6705, 222°) = (0.00, 0.044)	MGI No excess friction F0up = 9730 F0down = 720 F0 = 9010

Figure 9: IRIS Results: Mild Gas Interference Example 3

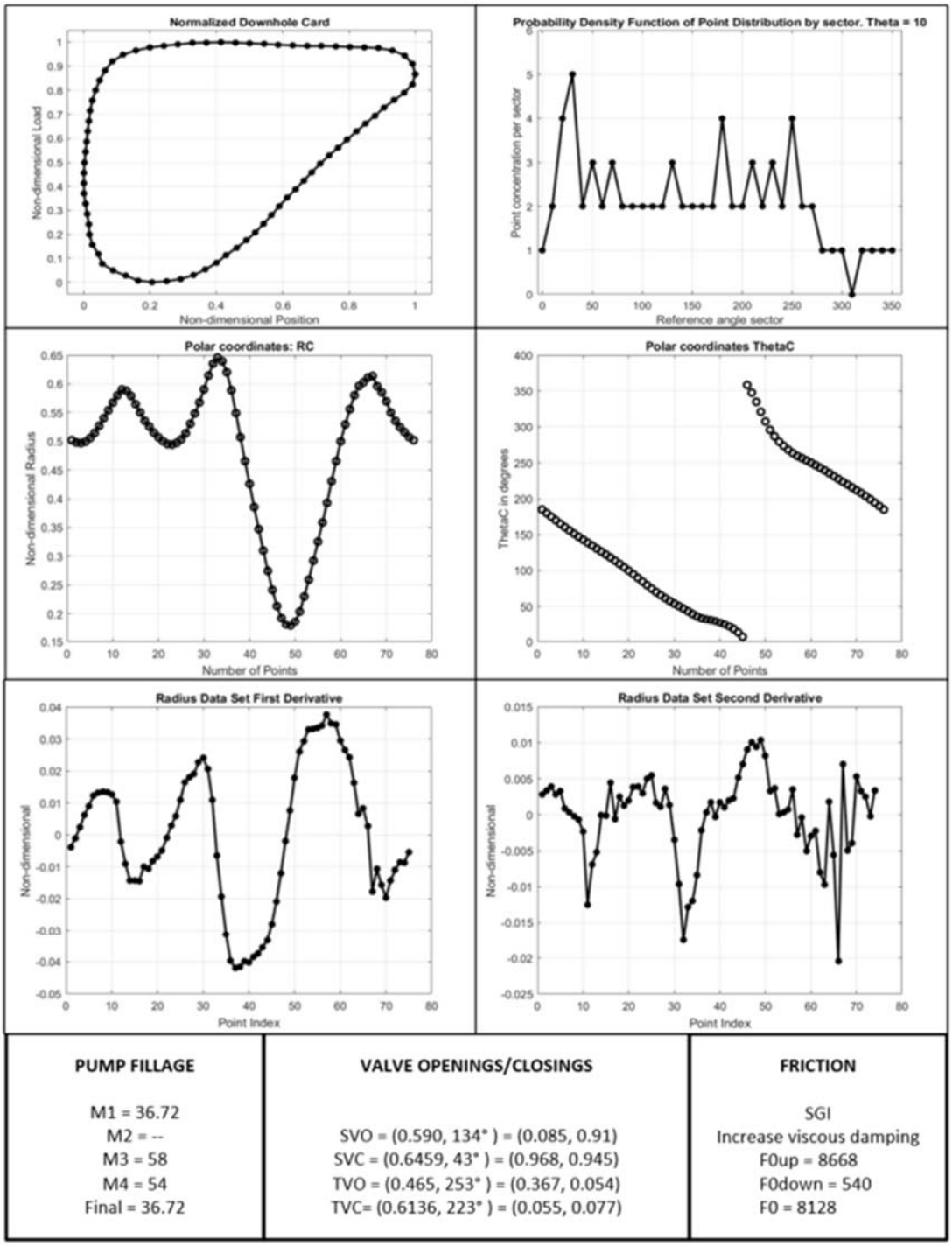

PUMP FILLAGE	VALVE OPENINGS/CLOSINGS	FRICTION
M1 = 36.72	SVO = (0.590, 134°) = (0.085, 0.91)	SGI
M2 = --	SVC = (0.6459, 43°) = (0.968, 0.945)	Increase viscous damping
M3 = 58	TVO = (0.465, 253°) = (0.367, 0.054)	F0up = 8668
M4 = 54	TVC= (0.6136, 223°) = (0.055, 0.077)	F0down = 540
Final = 36.72		F0 = 8128

Figure 10: IRIS Results: Severe Gas Interference Example 4

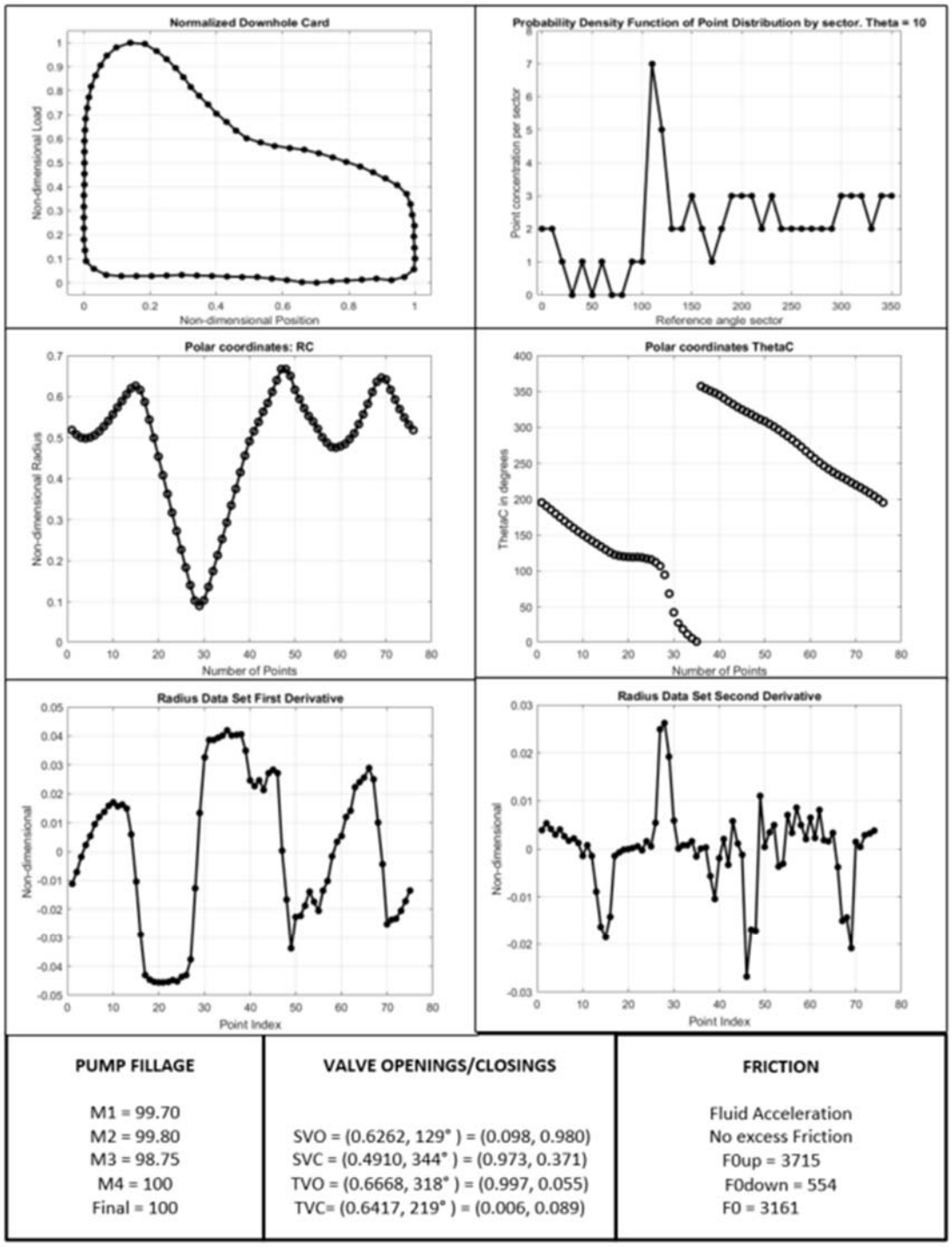

PUMP FILLAGE	VALVE OPENINGS/CLOSINGS	FRICTION
M1 = 99.70		Fluid Acceleration
M2 = 99.80	SVO = (0.6262, 129°) = (0.098, 0.980)	No excess Friction
M3 = 98.75	SVC = (0.4910, 344°) = (0.973, 0.371)	F0up = 3715
M4 = 100	TVO = (0.6668, 318°) = (0.997, 0.055)	F0down = 554
Final = 100	TVC= (0.6417, 219°) = (0.006, 0.089)	F0 = 3161

Figure 11: IRIS Results: Fluid Acceleration Example 5